

We are IntechOpen, the world's leading publisher of Open Access books Built by scientists, for scientists

6,900

Open access books available

186,000

International authors and editors

200M

Downloads

Our authors are among the

154

Countries delivered to

TOP 1%

most cited scientists

12.2%

Contributors from top 500 universities



WEB OF SCIENCE™

Selection of our books indexed in the Book Citation Index
in Web of Science™ Core Collection (BKCI)

Interested in publishing with us?
Contact book.department@intechopen.com

Numbers displayed above are based on latest data collected.
For more information visit www.intechopen.com



Adhesion Phenomenon of Liquid Metals

Hadeef Zakaria and Kamli Kenza

Abstract

In this chapter, we study an interfacial phenomenon between liquid metals and ceramic substrates. Therefore, investigation of these phenomena is of great importance not only in technological applications but also in fundamental understanding of physical behavior of the adhesion between two different materials as far as their electrical structures and physiochemical properties are concerned. Moreover, adhesion energy is interpreted thermodynamically by the interfacial interactions and the nature of bonding between liquid metal and ceramic material. The adhesion energy in metal/ceramic systems is determined by using an electro-acoustical model based on the propagation of the acoustic wave in the interface and strongly depends on the electric properties of combination.

Keywords: Liquid metal, Ceramics, Adhesion, Interfaces, Gap energy, Acoustic parameters

1. Introduction

Metalized ceramics by liquid metal have a crucial uses in several modern technological applications such as solar cell [1–4] electrical devices [5–7] and Micro Electro Mechanical Systems (MEMS) [8–10]. Recently, these systems are used as the conductive wiring of microelectronic circuits; there has been considerable interest in the characterization of the structure and properties of liquid metal/ceramic interface [11].

However, the coating of ceramic surfaces can affect most of the properties of the interface. Therefore, the investigation of interfacial phenomena between metals and ceramic substrates is of great importance not only in technological applications but also in fundamental understanding of physical behavior of the adhesion between two different materials as far as their electrical structures and physiochemical properties are concerned. In fact, at the interface of a metal/ceramic system, adhesion occurs when the atoms or molecules of the two contacting surfaces approach each other so closely that attractive forces between approaching atoms (or molecules) bond them together. The strength of the bond depends on the size of the atoms, the distance between them, and the presence or absence of contaminant matter on the surface [1]. Hence, the strength or weakness of bonds is the key factor to determine the interface stability: good adhesion, welded adhesion, perfect bonding, weak bonding smooth interface, etc. The metal/ceramic contact is characterized by the adhesion energy, W_{ad} , which is the work per unit area of the interface needed to separate reversibly a metal/ceramic interface [2]. This physicochemical

parameter is given by Young-Dupré equation relating surface tension of molten metal above melting temperature, γ_{LV} , and measured equilibrium contact angle θ formed between deposited liquid metal and its ceramic substrate [12]:

$$W_{ad} = \gamma_{LV} (1 + \cos\theta) \quad (1)$$

Adhesion energy represent in generally the sum of all interfacial interactions between two surfaces [13]:

$$W_{ad} = W_{non-equil} + W_{equil} \quad (2)$$

$W_{non-equil}$ and W_{equil} represents non-equilibrium and equilibrium contributions respectively of interfacial interactions. The first term does not exist in the absence of chemical reactions, and the second term corresponds to non-reactive metals/ceramic systems [13], this later expressed by:

$$W_{equil} = W_{VDW} + W_{chem-equil} \quad (3)$$

W_{VDW} is van der Waals interaction and $W_{chem-equil}$ is chemical equilibrium interactions accompanied by formation of these chemical bonds between two contact phases. It is imported to note that these interfacial bonds rested without rupture contrary in non-equilibrium systems [13]. Van der Waals energy in metal/ceramic systems estimate the can be numerically estimated by considering the dispersion interaction between a pair of atoms:

$$W_{VDW} = n \frac{3\alpha_M\alpha_C}{2R^6} \left[\frac{I_M I_C}{I_M + I_C} \right] \quad (4)$$

α_M and α_C are the polarizability volume of metal and ceramic; I_M and I_C the first ionization potential of metal atom and ceramic atom respectively. R is the distance between centers of the interacting atom.

At the interface zone, the surface acoustic wave (SAW) propagation which depends on elastic properties of solid substrates is greatly affected: the response would be different depending on the weakness or strength of bonds due to impedance mismatching [14]. Hence, in this context, we investigate the dependences of adhesion energy on acoustic parameters, in particular SAW velocities, for many metal/ceramic systems.

The objective of the electro-acoustic model [15] is the investigation of interfacial adhesion in liquid metal/ceramic systems subjected to non-reactive wetting in order to eliminate the non-equilibrium contribution $W_{non-equil}$ of adhesion work during a chemical reaction at the interface. A wide range of non-reactive liquid metals were used in this proposed model.

2. Choice of liquid metals

At the room temperature, most metals have a crystalline phase; the most widely used are iron, aluminum and copper. They are often present in oxide form (sodium oxide, magnesium oxide ...), some metals are present in the non-oxidized state (precious metals: platinum, gold) or in the form of alloys. Metal alloys are in general the combination of two or more metals as in the case of brasses (alloys of copper and zinc); but they can also contain non-metallic elements (i.e. iron-carbon alloy). Metals and their alloys are usually very good conductors of heat and electricity; they

are most often hard, rigid and plastically deformable. It should be noted that a large number of metals have a very high melting point, since they have relatively weak mechanical properties and are most often characterized by a wettability, a low thermal and electrical conductivity (as in the case of copper and gold). Therefore, the use of metals in metallized ceramic structures requires a fusion process in order to liquefy or melt these metals. For this, the role of metallization is to make the ceramic wettable by the liquid metal.

Several liquid metals parameters used in this investigation are listed in **Table 1**; sound velocities at melting temperatures are tabulated by Blairs [16], surface tension values are proposed by Keene [17], Liquid densities are taken by Crawley [18] and by Blairs [16]. Whiles the elastic constants, solid densities and Rayleigh velocity are obtained from Briggs [19].

Metal	c (m/s)	γ_{LV} (mJ/m ²)	P_{lm} (Kg/m ³)	T_f (K)	E (GPa)	ρ_{sm} (Kg/m ³)	V_{RM} (m/s)
Na	2526	203	951	371	10	968	1875
Mg	4065	577	1589	922	45	1738	2978
Al	4561	1075	2390	933	70	2700	3130
Si	6920	859	2524	1685	169	2330	4863
Ca	2978	362	1378	1112	20	1550	2203
Fe	4200	1909	7042	1809	211	7874	3003
Co	4031	1928	7740	1768	209	8900	2905
Ni	4047	1834	7889	1726	207	8908	2796
In	2337	561	7015	430	11	7310	766
Cu	3440	1374	8089	1357	130	8920	2159
Zn	2850	817	6552	693	108	7140	2148
Ga	2873	724	5900	303	10	5910	749
Ge	2693	631	5487	1210	89,6	5323	2057
Ag	2790	955	9329	1234	83	10490	1658
Cd	2256	637	7997	594	51	8650	1446
Sn	2464	586	6973	505	50	7310	1400
Sb	1900	382	6077	904	55	6697	1540
Ba	1331	273	3343	1002	13	3510	1020
La	2030	728	5940	1193	37	6146	1443
Ce	1694	750	6550	1071	34	6689	1318
Pr	1926	716	6500	1204	37	6640	1380
Yb	1274	320	6720	1097	24	6570	1013
Ta	3303	2083	14353	3287	186	16650	2082
Pt	3053	1746	18909	2042	168	21090	1924
Au	2568	1162	17346	1336	78	19300	1536
Sc	4272	939	2680	1812	74	2985	3039
Ti	4309	1475	4141	1943	116	4507	3061
V	4255	1856	5340	2175	128	6110	2831
Y	3258	872	4180	1799	64	4472	2263
Zr	3648	1463	5650	2125	68	6511	2406

Metal	c (m/s)	γ_{LV} (mJ/m ²)	ρ_{lm} (Kg/m ³)	T_f (K)	E (GPa)	ρ_{sm} (Kg/m ³)	V_{RM} (m/s)
Nb	3385	1757	7830	2740	105	8570	2406
Pb	1821	471	10587	601	16	1146	2118
Pd	2657	1482	10495	1825	117	12023	742
Hf	2559	1517	11550	2500	78	13310	1789
Nd	2212	685	6890	1289	41	6800	1503
Sm	1670	431	7420	1345	50	7353	1411
Eu	1568	264	5130	1090	18	5244	1301
Gd	2041	664	7790	1585	55	7901	1083
Tb	2014	669	8050	1630	56	8219	1537
Dy	1941	648	8370	1682	61	8551	1525
Ho	1919	650	8580	1743	65	8795	1561
Er	1867	637	8860	1795	70	9066	1592
Lu	2176	940	9750	1936	69	9841	1426

Table 1.
Experimental sound velocities, c , surface tensions, σ_m , densities, ρ_{lm} of different liquid metals at the melting temperature, elastic moduli, E , solid density, ρ_{sm} , and calculated Rayleigh velocities, V_R of these metals at solid state.

3. Relationship between the properties of metals in solid and liquid states

Analytical study has been proposed to express the relation between experimental sound velocities of liquid metals at the melting temperature, c , and determinate

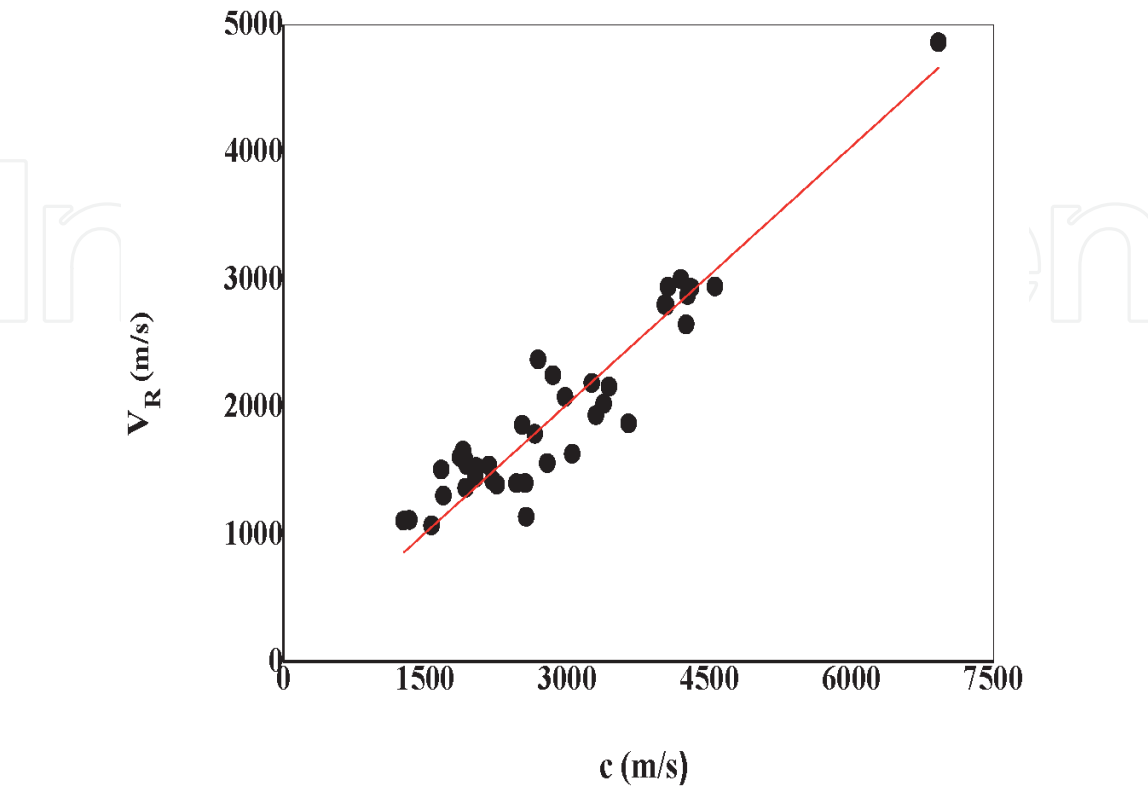


Figure 1.
Correlation between experimental sound velocities of liquid metals and Rayleigh velocities of these metals in solid state [20].

acoustic velocities, V_R , of these metals at solid state by SAM technique. The variation of V_R -values as function of c was made; it shows a linear increase of V_R with c increasing. Simple fitting was made and resulted in a well-defined linear correlation between the quantities, as can be seen in **Figure 1**.

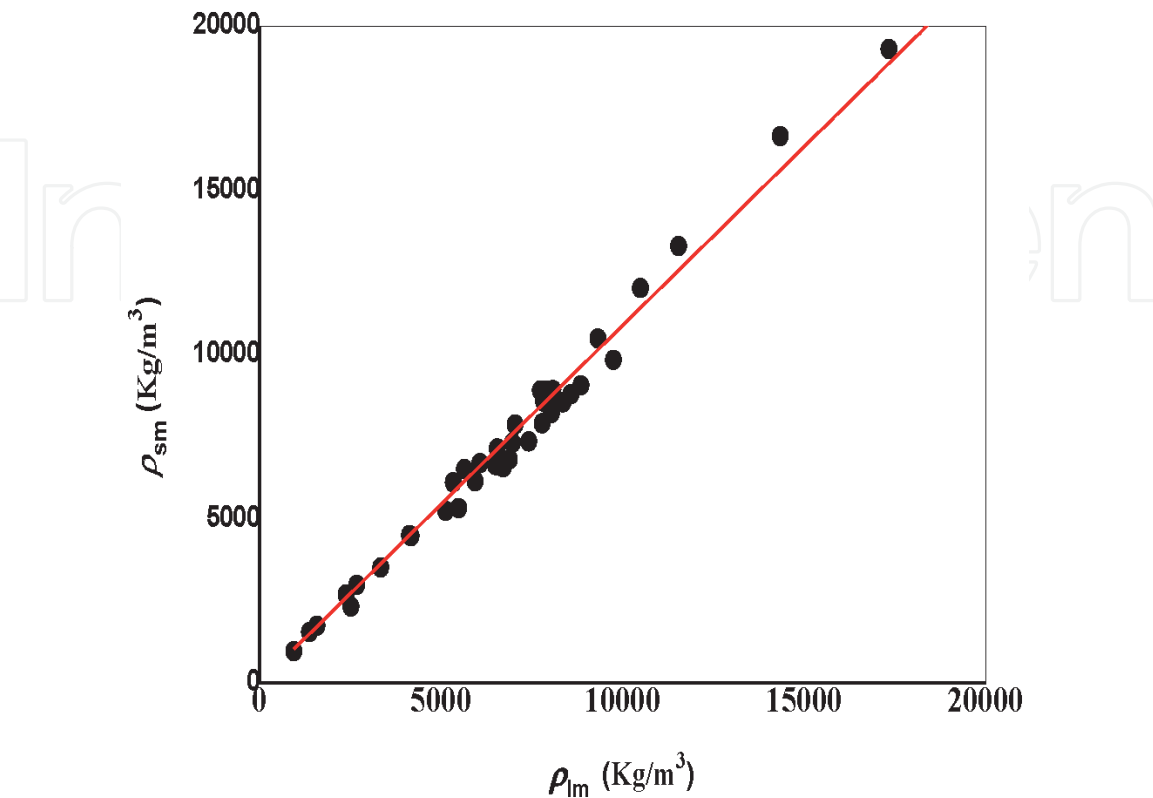


Figure 2.
Correlation between liquid and solid densities of metals [20].

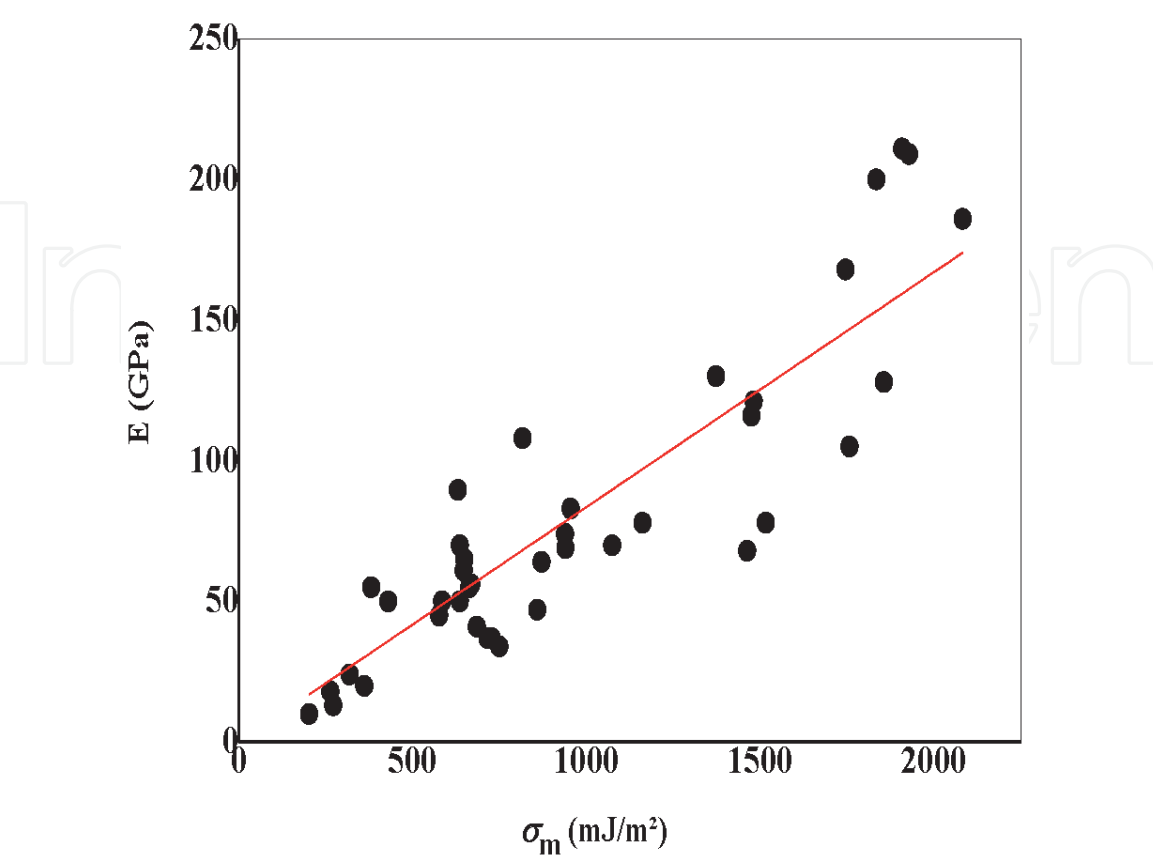


Figure 3.
Correlation between Young's moduli and surface tension of liquid metals [20].

Relationship between these parameters can be quantified by the following equation:

$$V_R = 0.674 \, c \tag{5}$$

One can see also a clear tendency between the liquid metals densities, ρ_{lm} , with that of these metals at solid state, ρ_{sm} , as can be seen in **Figure 2**.

The relationship that expresses this tendency can take the following form:

$$\rho_{sm} = 1.088 \, \rho_{lm} \tag{6}$$

A close comparative between one of very important properties of liquid metal, which is the surface tension, σ_m , and Young's moduli, E , values shows a linier dependence between these parameters, as can be seen in **Figure 3**.

To quantify the relationship between elastic moduli and surface tension, a simple plot was made; a linear correlation is defined, that it can be written as:

$$E = 0.083 \, \sigma_m \tag{7}$$

The importance of the Eqs. (5)-(7) lies in the prediction of acoustic parameters from liquid to solid states of metals and vice versa.

4. Determination of adhesion energy in liquid metal/ceramic systems

Very recently, an electro-acoustical model [15] has been proposed to estimate and interpreted the work of adhesion of non-reactive liquid metal/ceramic substrates systems in terms of the Rayleigh velocity of acoustic wave propagation in surface of all types of corresponding ceramic substrates, V_{RC} .

In this model, several metals are considered (Au, Cu, Sn, Ga and Ag) on a great number of ceramic substrates (AlN, Al₂O₃, BN, CoO, Er₂O₃, Ho₂O₃, Lu₂O₃, MgO, NiO, SiC, SiO₂, TiC, TiO, TiO₂, Ti₂O₃, Y₂O₃, Yb₂O₃, ZnO and Zr₂O₃). The characteristics of all ceramic materials: energy gap, E_g [21] density, ρ_C , Young's modulus, E_C , and Rayleigh velocities [19] are listed in **Table 2**.

Ceramics Substrate	E_g (eV)	ρ_C (kg/m ³)	E_C (GPa)	V_{RC} (m/s)
AlN	5.6	3260	318	5616
Al ₂ O ₃	7.1	3980	330	5650
BN	8.1	3487	34	1834
CoO	0.5	9423	281	2871
Er ₂ O ₃	3.2	8651	179	2633
Ho ₂ O ₃	3.9	8414	175	2639
Lu ₂ O ₃	4.0	9423	204	2691
MgO	7.3	3580	310	5297
NiO	2.5	6670	420	6205
SiC	3.3	3210	393	6714
SiO ₂	7.9	2600	75	3678
TiC	0.3	4940	400	5370

Ceramics Substrate	E_g (eV)	ρ_C (kg/m ³)	E_C (GPa)	V_{RC} (m/s)
TiO	0.0	4950	387	3960
TiO ₂	3.1	4230	315	4917
Ti ₂ O ₃	0.1	4468	118	4411
Y ₂ O ₃	5.5	5030	176	3398
Yb ₂ O ₃	1.4	9293	229	2677
ZnO	3.4	5606	125	2730
ZrO ₂	8.0	5600	244	3781

Table 2.
Characteristics of investigated ceramic materials: energy gap, E_g , density, ρ_C and Young’s modulus, E_C , and determined Rayleigh velocities, V_{RC} .

The variations of work of adhesion on Rayleigh velocity for different ceramic substrate, V_{RC} , in contacting with different non-reactive metals (Au, Cu, Sn, Ga and Ag) are investigated. In this study, some published data on wok of adhesion for different metals/ceramics systems are considered [12, 13, 22–34].

In the first time liquid gold/ceramic combinations are taken the obtained results are illustrated in **Figure 4**.

In order to generalize the above observations obtained with liquid Gold/ceramic systems and to put into evidence the results reproducibility, several other nonreactive metals deposited in different ceramic substrates are considered, i.e., (Cu, Sn, Ga and Ag):

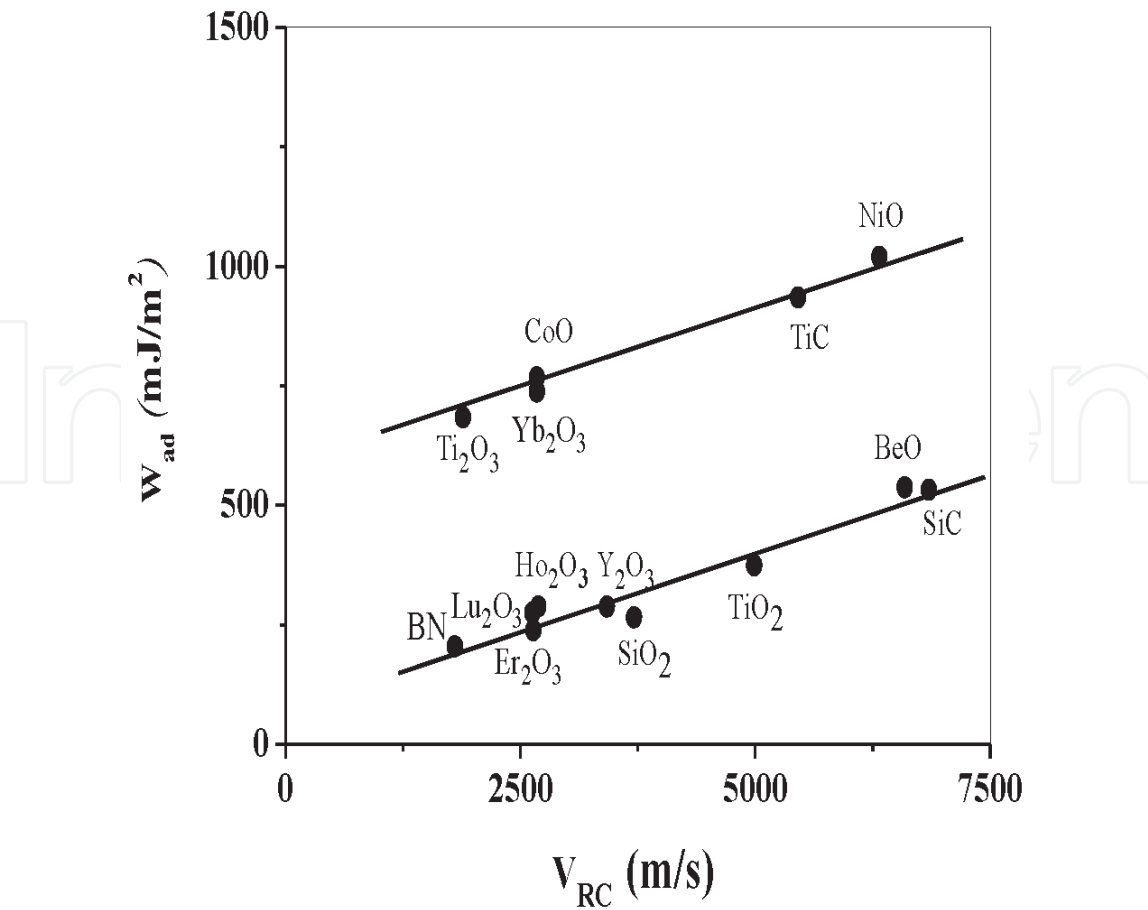


Figure 4.
Work of adhesion as function of calculated Rayleigh velocities of different ceramic substrates in contacting with gold [15].

The obtained results are illustrated in **Figure 5** in terms of work of adhesion as a function of ceramic Rayleigh velocities in contacting with several non-reactive metals. All the curves show the same behavior: the work of adhesion increases linearly with increasing V_{RC} . However, two sets of linear dependences are distinguished that are regrouped according to the band gap energy of the ceramic substrate, as discussed below.

The dependence of W_{ad} on V_{RC} (Au) is quantified via curve fitting, (lines in **Figures 4** and **5**). We distinguish two parallel dependences for gold/ceramic substrate systems: for higher energy values (upper curve) the linear variation is found to be of the form:

$$W_{ad}(Au) = 0.07V_{RC} + 553 \quad (8)$$

Whereas, for small energy values (lower curve), the linear dependence is found to be of the form:

$$W_{ad}(Au) = 0.07V_{RC} + 76 \quad (9)$$

Moreover, it should be noted that the same behavior of two parallel lines is obtained for all metal/ceramic systems. Therefore, all curves have a same slop not only for small gap materials but also for large gap ceramics; the general expression takes the form:

$$W_{ad}(Me) = 0.07 V_{RC} + C \quad (10)$$

$$W_{ad}(Me) = 0.07 V_{RC} + C' \quad (11)$$

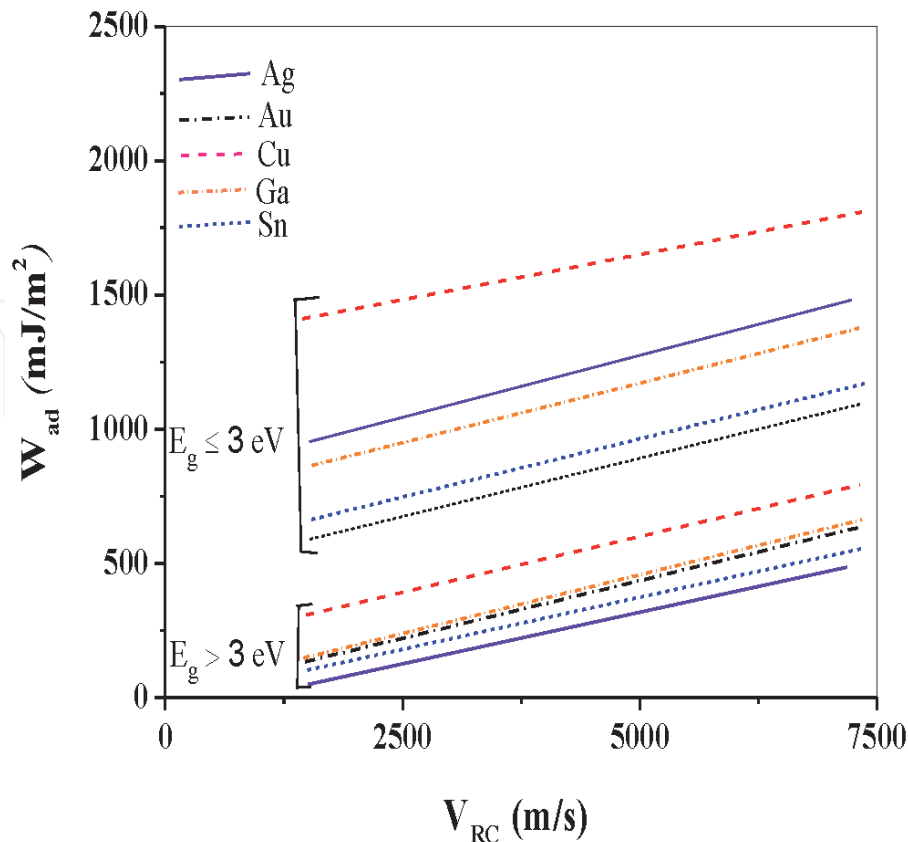


Figure 5. Work of adhesion as function of calculated Rayleigh velocities of different ceramic substrates in contacting with several metals [15].

where the subscript, (Me), represents any given investigated nonreactive liquid metal (Ag, Au, Cu, Ga and Sn), C and \hat{C} are characteristic constants for each metal/ceramic combination.

The exact corresponding values of characteristic constants C (for small gap ceramic materials) and \hat{C} (for large gap ceramic materials) of several liquid metal/ceramic systems are giving in the **Table 3**.

The similar dependence (with the same slope equal to $0.07V_{RC}$) is indicative of the existence of the same mechanism responsible for this behavior. However the existence of two parallel dependences for every system is due to the energy band structure of the ceramic materials in particular the energy gap (**Table 1**). A close analysis of **Figure 5** and the E_g column clearly shows that the upper set of curves corresponds to solid ceramic materials with small energy gaps ($E_g \leq 3$ eV), whereas the lower ensemble of curves represents ceramic materials with large energy gaps ($E_g > 3$ eV).

In fact, solid materials with small band gaps behave as conductors ($E_g \rightarrow 0$) or semiconductors ($E_g \leq 3$ eV). In this case, it was reported [35] that the high adhesion energy values of same metal/ceramic systems are associated with high electron density of metals and low band gap energy of solids ceramics. The interfacial adhesion between a metal and a ceramic crystal is assured by the electron transfer [12], it is interesting to define an interfacial propriety represents the minimum energy needed for appearance of a limit number of interfacial bonds responsible for generating of the adhesion between the metal and the ceramic, this energy is caused by Van der Waals interaction, W_{VDW} . The intensity of the electron transfer at small band gap solid ceramic is increased because of its wealth by the free charges inside and the chemical equilibrium contribution $W_{chem-equil}$ taking place.

For large band gaps, there will be practically a small number of free charges inside in the ceramic crystal. As a result, the chemical equilibrium contribution $W_{chem-equil}$, to the adhesion energy is negligible. Consequently, the adhesion energy is approximately resulted by from the Van der Waals interaction [12].

The Van der Waals contribution of adhesion energy rested constant and proportional with Rayleigh velocity of ceramic materials whether it is the band gap energy, for the first time it is determined exactly as follows:

$$W_{VDW} = 0.07 V_{RC} \tag{12}$$

The determinate W_{VDW} energy values for different metal/ceramic systems depend directly on the choice of various parameters appearing in Eq. (3). For example, Mc Donald and Eberhart [36] calculated W_{VDW} values equal to 500 ± 150 mJ/m² for different metal/alumina systems, that in our model and for the same system we have found W_{VDW} values equal to 396 mJ/m². While Naidich [13] found W_{VDW} values of 350 150 mJ/m² for metal/oxide ceramic systems, this

Metals	C (mJ/m ²)	\hat{C} (mJ/m ²)
Ag	991	14
Au	533	76
Cu	1309	228
Ga	863	78
Sn	602	37

Table 3.
C and \hat{C} values of different liquid metal/ceramic system.

confirms the compatibility between our proposed model and other model of W_{VDW} estimation.

For small gap ceramic materials, the characteristic constant C of Eq. (10) represents $W_{chem-equil}$ contribution, this energy is relatively important compared to W_{VDW} energy, it represents another interfacial property responsible for putting the stability and the perfection to the interface between metal and ceramic. The good convergence in $W_{chem-equil}$ values for a given metal/small gap ceramics could be explained by the fact that for ($E_g < 3$ eV), here will be a big density of inside in the ceramic crystal and consequently height electron transfer.

In this work, an analytical approach [20] is adopted to express the relation between experimental sound velocities of liquid metals, c , at the melting temperature and determinate Rayleigh velocity of these metals at solid state, V_{RM} , by SAM program. Hence, V_{RM} is expressed in terms of c , as we recently reported [20].

$$V_{RM} = 0.674 \, c \tag{13}$$

The determinate chemical equilibrium energy, $W_{chem-equil}$ of metal/small band gap ceramic system by Eq. (10) are summarized in **Table 4**.

The variations of chemical equilibrium energy on normalized Rayleigh velocity, (V_{RM}/z) for different bulk metals in contacting with several small band gap ceramic materials are investigated, where z is number of coordination's of each metal atom. In this investigation, we consider Eq. (10) to determine $W_{chem-equil}$ and some published wok on adhesion energy for different metals/ceramics systems [12, 13, 22–34]. The obtained results are presented below.

The dependence of $W_{chem-equil}$ on (V_{RM}/z) is quantified via curve fitting, (line in **Figure 6**). We distinguish dependence for liquid metal/small band gap ceramic substrate systems: the linear variation is found to be of the form:

$$W_{chem-equil} = (1.3/z)V_{RM} \tag{14}$$

So, the chemical equilibrium contribution of adhesion energy in metal/ceramic system is related directly to the Rayleigh velocity of metals.

For large gap ceramic materials, the discrepancy in \hat{C} values for a given metal/large gap ceramics could be explained by the fact that for ($E_g > 3$ eV), here will be a

Metals	$W_{chem-equil}$ (mJ/m^2)	Z
Ag	991	2
Al	1269	3
Au	553	3
Cu	1309	2
Co	1341	3
Fe	1276	3
In	723	3
Ni	1193	3
Ga	863	3
Sn	602	4

Table 4.
Determinate chemical equilibrium energy, $W_{chem-equil}$ of metal/small band gap ceramic system and the number of coordination's of each atom of metal, z .

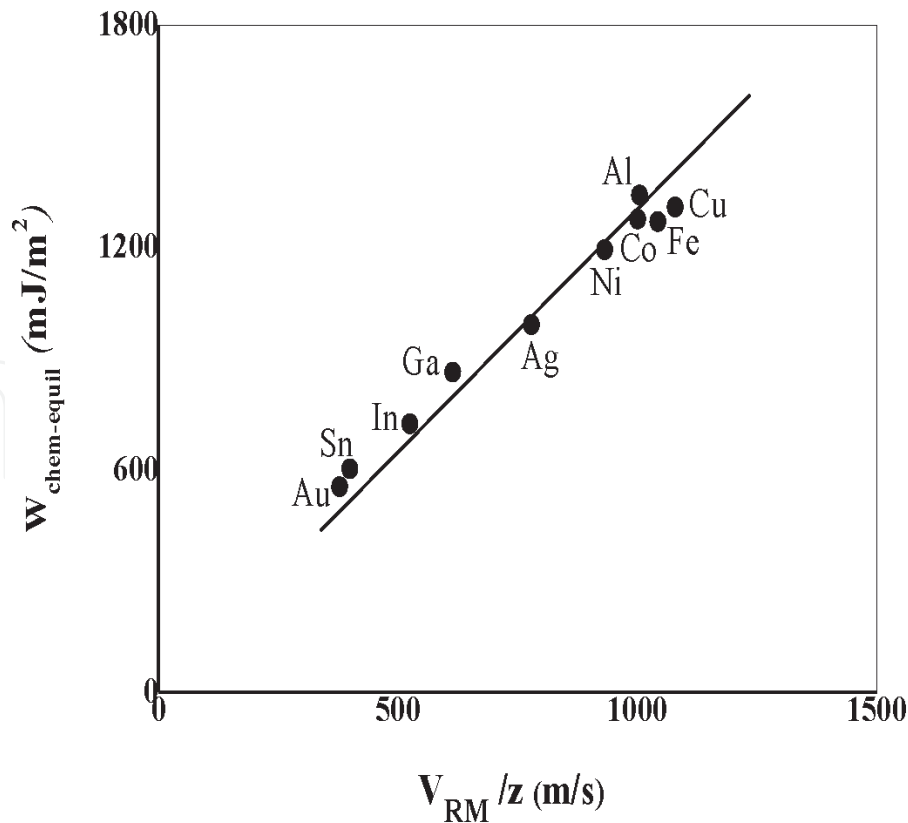


Figure 6.
Chemical equilibrium energy of metal/small band gap ceramic system as function of normalized Rayleigh velocities of different bulk metals [15].

smaller density of inside in the ceramic crystal (practically no free charges inside) and consequently the electron transfer at metal/ceramic interfaces cannot be important [2]. As a result, the characteristic constant \hat{C} values are negligible compared to W_{VDW} energy and/or especially to $W_{chem-equil}$ energy.

Therefore, the general expression of adhesion energy takes the form:

a. For small gap ceramic materials:

$$W_{ad} (Me) = 0.07 V_{RC} + (1.3/z) V_{RM} \tag{15}$$

b. For large gap ceramic materials:

$$W_{ad} (Me) = 0.07 V_{RC} + W_{negl} \tag{16}$$

The importance of the deuced relation lies in its applicability to all investigated metal/ceramic systems. It could be extended, through familiar relations, to other acoustic parameters. Similar results for longitudinal and transverse velocities were obtained. Moreover, preliminary results for elastic constants (Young's modulus and shear modulus) are very satisfying.

5. Conclusions

In this work, an interfacial phenomenon between liquid metals and ceramic substrates has been investigated. Moreover, same liquid metal characteristics (sound velocity propagation in liquid metal, liquid density and surface tension) were predicted by the metal characteristics in solid state (Rayleigh velocity, solid

density and Young's modulus). Adhesion energy terms in metals/ceramic systems were determined by using an electro-acoustic model. It was shown that the adhesion energy increases linearly with Rayleigh velocity of ceramic substrates for all types of ceramics. Van der Waals term of adhesion energy was deduced only depends on Rayleigh velocities of ceramic. On the other hand, the chemical equilibrium term was deduced strongly depends on the energy gap of the ceramics materials: it was higher for small band gap ceramic materials and depends on Rayleigh velocities of metals, for the opposite case it was deduced negligible. These universal relations that could be extended to other acoustic parameters are applicable to all metal/ceramic combinations.


Author details

Hadef Zakaria* and Kamli Kenza

Department of Physics, Faculty of Sciences, University 20 Août 1955-Skikda, Skikda, Algeria

*Address all correspondence to: zaki-hd2013@yahoo.fr; z.hadef@univ-skikda.dz

IntechOpen

© 2021 The Author(s). Licensee IntechOpen. This chapter is distributed under the terms of the Creative Commons Attribution License (<http://creativecommons.org/licenses/by/3.0>), which permits unrestricted use, distribution, and reproduction in any medium, provided the original work is properly cited. 

References

- [1] Gordon I, Van Gestel D, Van Nieuwenhuysen K, Carnel L, Poortmans J. Thin-film polycrystalline silicon solar cells on ceramic substrates by aluminium-induced crystallization, *Thin Solid Films*, 2005;487: 113-117. <https://doi.org/10.1016/j.tsf.2005.01.047>
- [2] Tabrizia AA, Pahlavan A. Efficiency, improvement of a silicon-based thin-film solar cell using plasmonic silver nanoparticles and an antireflective layer, *Optics Communications*, 2020; 454: 124437. <https://doi.org/10.1016/j.optcom.2019.124437>
- [3] Yan D, Phang SP, Wan YM, Samundsett C, Macdonald D, Cuevas A. High efficiency n-type silicon solar cells with passivating contacts based on PECVD silicon films doped by phosphorus diffusion, *Solar Energy Materials and Solar Cells*, 2019;193: 80-84. <https://doi.org/10.1016/j.solmat.2019.01.005>
- [4] Shao X, XiS, Li G, Liu Peng R, Li C, Chen G, ChenR. Longer hydrogenation duration for large area multi-crystalline silicon solar cells based on high-intensity infrared LEDs, *Optics Communications*, 2019; 450: 252-260. <https://doi.org/10.1016/j.optcom.2019.06.011>
- [5] Legallais M, Thu T, Nguyen T, Cazimajou T, Mouis M, SalemB, Ternon C, Material engineering of percolating silicon nanowire networks for reliable and efficient electronic devices, *Materials Chemistry and Physics*, 2019;238: 121871, <https://doi.org/10.1016/j.matchemphys.2019.121871>
- [6] Zhang X, Feng M, Zhao M, Zhang P, He C, Qi H, Han W, Guo F, Failure of silicon nitride ceramic flotation spheres at critical state of implosion, *Applied Ocean Research*, 2020;97: 102080 <https://doi.org/10.1016/j.apor.2020.102080>
- [7] Bulyarskiy SV, The effect of electron-phonon interaction on the formation of reverse currents of p-n-junctions of silicon-based power semiconductor devices, *Solid-State Electronics*, 2019; 160: 107624. <https://doi.org/10.1016/j.sse.2019.107624>
- [8] Wang J, Wu L, Chen X, Zhuo W, Avoiding blister defects in low-stress hydrogenated amorphous silicon films for MEMS sensors, *Sensors and Actuators A: Physical*, 2018; 276: 11-16. <https://doi.org/10.1016/j.sna.2018.04.021>
- [9] Jantawong J, Atthi N, Leepattarapongpan C, Srisuwan A, Jeamsaksiri W, Sooriakumar K, Austin A, Niemcharoena S, Fabrication of MEMS-based capacitive silicon microphone structure with staircase contour cavity using multi-film thickness mask, *Microelectronic Engineering*, 2019; 206: 17-24. <https://doi.org/10.1016/j.mee.2018.12.004>
- [10] Almuramady N, Borodich, Feodor MB, Goryacheva I, Torskaya EV, Damage of functionalized self-assembly monomolecular layers applied to silicon microgear MEMS, *Tribology International*, 2018; 129: 202-213. <https://doi.org/10.1016/j.triboint.2018.07.049>
- [11] Frear D, Packaging Materials, Eds, Springer Handbook of Electronic and Photonic Materials, Springer Handbooks. Springer, Cham; 2017, https://doi.org/10.1007/978-3-319-48933-9_53
- [12] Li JG, Chemical trends in the thermodynamic adhesion of metal/ceramic systems, *Mater. Lett.* 1995; 22: 169-174. [https://doi.org/10.1016/0167-577X\(94\)00244-4](https://doi.org/10.1016/0167-577X(94)00244-4)
- [13] Naidich YV, The wettability of solids by liquid metals, *Progr. Surf.*

- Membr. Sci., 1981; 14:353-486. <http://dx.doi.org/10.1016/B978-0-12-571814-1.50011-7>
- [14] Viktorov IA, Rayleigh and Lamb Waves, Plenum Press, New York, 1967.
- [15] Kamli K, Hadeef Z, Gacem A, Houaidji N. Prediction of Adhesion Energy Terms in Metal/Ceramic Systems by Using Acoustic Parameters, Metallophysics and Advanced Technologies, 2020; 42(5): 717-730. <https://doi.org/10.15407/mfint.42.05.0717>
- [16] Blairs S, Correlation between surface tension, density, and sound velocity of liquid metals, Coll. Inter. Sci., 2006; 302: 312-314. <https://doi.org/10.1016/j.jcis.2006.06.025>
- [17] Keene BJ, Review of data for the surface tension of pure metals, Int. Mat. Rev., 1993; 38: 157-192. <https://doi.org/10.1179/imr.1993.38.4.157>
- [18] Crawley AF, Densities of Liquid Metals and Alloys, Int. Met. Rev., 1974; 19: 32-48. <https://doi.org/10.1179/imttr.1974.19.1.32>
- [19] Briggs GAD, Kolosov OV, Acoustic Microscopy, Oxford Univ. Press, 2nd Edition, New York, 2010. DOI:10.1093/acprof:oso/9780199232734.001.0001
- [20] Hadeef Z, Doghmane A, Kamli K, Hadjoub Z, Correlation between surface tension, work of adhesion in liquid metals/ceramic systems and acoustic parameters, Progress in Physics of Metals, 2018; 19(2): 198-223. <https://doi.org/10.15407/ufm.19.01.198>
- [21] Strehlow WH, Cook EL, Compilation of Energy Band Gaps in Elemental and Binary Compound Semiconductors and Insulators, J. Phys. Chem. Ref. Data, 1973; 2: 163-199. <https://doi.org/10.1063/1.3253115>
- [22] Eustathopoulos N, Sobczak N, Passerone A, Nogi K. Measurement of contact angle and work of adhesion at high temperature, Mater. Sci., 2005; 40: 2271-2280. <https://doi.org/10.1007/s10853-005-1945-4>
- [23] Naidich YV, Zhuravlev VS, Frumina NI, Wetting of rare-earth element oxides by metallic melts, Mater. Sci., 1990; 25: 1895-1901. <https://doi.org/10.1007/BF01045739>
- [24] Li JG, Wettability of Solid Inorganic Materials by Gold, Scripta Metall. Mater., 1994; 30: 337-342. [https://doi.org/10.1016/0956-716X\(94\)90385-9](https://doi.org/10.1016/0956-716X(94)90385-9)
- [25] Taranets NY, Naidich YV, Wettability of aluminum nitride by molten metals, Powder Metall. Met. Ceramics, 1996; 35: 74-78. <https://doi.org/10.1007/BF01328834>
- [26] Liu GW, Muolo ML, Valenza F, Passerone A, Survey on wetting of SiC by molten metals, Ceram. Inter., 2010; 36: 1177-1188. <https://doi.org/10.1016/j.ceramint.2010.01.001>
- [27] Kida M, Bahraini M, Molina JM, Weber L, Mortensen A, High-temperature wettability of aluminum nitride during liquid metal infiltration, Mater. Sci. Eng. A, 2008; 495: 197-202. <https://doi.org/10.1016/j.msea.2007.12.050>
- [28] Naidich YV, About liquid metal/ceramic interface interaction mechanism and mode of a new intermediate compound formation, Curr. Opi. Sol. Sta. Mater. Sci., 2005: 161-166. <https://doi.org/10.1016/j.cossms.2005.11.001>
- [29] Li JG, Wetting and Interfacial Bonding of Metals with Ionocovalent Oxides, J. Amer. Ceram. Soc., 1992; 75: 3118-3126. <https://doi.org/10.1111/j.1151-2916.1992.tb04396.x>
- [30] Li JG, Hausner H, Contact angle and work of adhesion isotherms of silicon-tin alloys on monocrystalline silicon carbide, Mater. Let., 1991; 11: 355-357.

[https://doi.org/10.1016/0167-577X\(91\)90133-Q](https://doi.org/10.1016/0167-577X(91)90133-Q)

[31] Li JG, Wetting and interfacial bonding in liquid metal/solid ceramic systems, *Comp. Interf.*, 1993; 1: 37-53. <https://doi.org/10.1163/156855493X00301>

[32] Li JG, Hausner H, Wetting and adhesion in liquid silicon/ceramic systems, *Mater. Letters*, 1992; 14: 329-332. [https://doi.org/10.1016/0167-577X\(92\)90047-N](https://doi.org/10.1016/0167-577X(92)90047-N)

[33] Chatain D, Rivollet I, Eustathopoulos N, Adh sion thermodynamique dans les syst mes non-r actifs m tal liquide-alumine, *Chim. Phys.*, 1986; 83: 561-567. <https://doi.org/10.1051/jcp/1986830561>

[34] Sotiropoulou D, Nikolopoulos P, Work of adhesion in ZrO₂-liquid metal systems, *J. Mater. Sci.*, 1993; 28: 356-360. <https://doi.org/10.1007/BF00357807>

[35] Li JG, Role of electron density of liquid metals and band gap energy of solid ceramics on the work of adhesion and wettability of metal-ceramic systems, *Mater. Sci. Let.*, 1992; 11: 903-905. <https://doi.org/10.1007/BF00729089>

[36] Mc Donald JB, Eberhart JG. Adhesion in aluminum oxide-metal systems, *Trans. AIME*, 1965; 233: 512-517.